

# An RF/Microwave Microfluidic Sensor Based on a 3D Capacitive Structure with a Floating Electrode for Miniaturized Dielectric Spectroscopy

Michael A. Suster<sup>1</sup>, Brecken Blackburn<sup>2</sup>, Umut Gurkan<sup>3</sup>, and Pedram Mohseni<sup>1</sup>

<sup>1</sup>Department of Electrical Engineering and Computer Science, Case Western Reserve University, Cleveland, OH USA

<sup>2</sup>Department of Electrical and Computer Engineering, Cornell University, Ithaca, NY USA

<sup>3</sup>Department of Mechanical and Aerospace Engineering, Case Western Reserve University, Cleveland, OH USA

**Abstract**—This paper reports on the design, fabrication and testing of a microfluidic sensor for a miniaturized measurement platform dedicated to dielectric spectroscopy at RF/microwave frequencies. The sensor employs a novel, three-dimensional, parallel-plate, capacitive sensing structure with a floating electrode integrated onto a PMMA microfluidic cap used for delivering the material-under-test (MUT) with a 9 $\mu$ L-sample volume. Requiring only an  $S_{11}$  measurement and after a 6-point calibration, complex relative permittivity readings by the sensor in the frequency range of 14MHz to 6.5GHz agree very well with bulk-solution reference measurements conducted with an *Agilent 85070E* dielectric probe kit. Using ethanol and ethylene glycol as two different MUTs with the sensor, the rms errors in real and imaginary parts of the complex relative permittivity of ethanol over the full frequency range are 3.5% and 5.6%, respectively. The corresponding numbers for ethylene glycol are 5.4% and 4.5%, respectively.

**Keywords**—Capacitive sensor, dielectric spectroscopy, microfluidics, miniaturized platform, RF/microwave sensor

## I. INTRODUCTION

Quantitative measurement of the complex dielectric permittivity of a material versus frequency (i.e., dielectric spectroscopy, or DS) is a powerful monitoring technique [1] with a broad range of applications including chemical analysis in the petroleum industry [2], soil moisture monitoring [3], pharmaceutical drug development [4] and proteomics research for the study of molecular dynamics and protein interactions [5], [6]. DS is also a powerful analytical tool in the biomedical field [7] as a label-free, non-destructive and real-time method to study key molecular characteristics of biomaterials for potential applications in disease detection and clinical diagnosis [8], [9].

Miniaturized DS sensors have been developed by combining a coplanar waveguide (CPW) and a microfluidic channel for sample delivery [10], [11]. As compared to commercial DS systems (e.g., *Agilent 85070E* dielectric probe kit) requiring bulk-solution measurements, these sensors need only a small liquid volume ( $\mu$ L to nL) confined to their microfluidic channel. However, these sensors still require an expensive microwave probe station to contact the sensor at the wafer level and a benchtop vector network analyzer (VNA) to perform two-port, S-parameter measurements for dielectric extraction.

Such a measurement setup is clearly not conducive to performing rapid, high-throughput and low-cost measurements using an autonomous, small-sized, low-power and portable instrument that might ultimately pave the way for translating DS measurements from the lab bench to the field for industrial applications or to the bedside for point-of-care diagnostics.

Recent efforts in miniaturizing the entire DS measurement platform include an on-chip, comb-finger, capacitive DS sensor (without microfluidic sample delivery) embedded in a 7-to-9-GHz voltage-controlled oscillator [12], or in a CMOS receiver integrated circuit (IC) for complex permittivity measurements in 0.62–10GHz [13]. A DS system based on an on-chip CPW transmission line embedded in a microfluidic channel and an integrated CMOS receiver IC has also been developed for complex permittivity measurements in 1–50GHz [14]. However, these systems integrate only the receiver circuitry, and thus still require a benchtop signal generator to drive the sensor. Furthermore, these systems currently do not operate in a frequency range-of-interest extending from low-MHz to several GHz, suitable for capturing the dielectric relaxation characteristics of a material-under-test (MUT) in  $\beta$ ,  $\delta$  and  $\gamma$  dispersion regions [7].

A miniaturized measurement platform for broadband DS studies in the range of MHz to GHz is conceptually illustrated in Fig. 1. We have previously reported a CMOS receiver IC for miniaturized dielectric spectroscopy that implemented a broadband frequency response analysis method [15], as well as a DS sensor based on a center-gapped microstrip line that was capable of measuring only the real part of complex relative permittivity in 14MHz–4GHz [16]. This paper reports on the design, fabrication and measured results of a new microfluidic sensor based on a novel, three-dimensional (3D), parallel-plate, capacitive sensing structure with a floating electrode that can accurately measure both real and imaginary parts of the complex relative permittivity in 14MHz–6.5GHz.

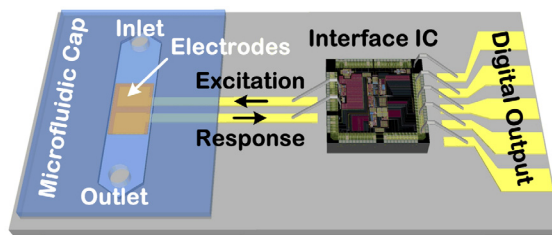


Fig. 1. Conceptual illustration of a miniaturized measurement platform for RF/microwave dielectric spectroscopy.

## II. SENSOR DESIGN

Planar electrodes have been recently used to implement DS sensors in the form of comb-finger, capacitive structures [12], [13] or CPWs [14]. An advantage of the planar approach compared to a 3D parallel-plate structure is the reduced fabrication requirements of routing all signals on a single layer, which facilitates the integration of the planar structure onto the surface of a printed-circuit board (PCB) or IC. However, DS sensors based on a planar structure rely on fringe electric (E) fields for the measurement of the MUT placed on the sensor top surface, hence requiring the MUT to be in direct contact with the metal electrode to achieve high sensitivity. A surface coating would increase the distance between the MUT and sensor, hence reducing the E-field strength and sensitivity. The constant E-field in a parallel-plate, capacitive sensing area solves this problem, but has not been widely implemented due to its fabrication complexity.

Fig. 2 shows both cross-sectional and top views of the proposed parallel-plate, capacitive sensor based on a novel 3D-gap with a floating electrode that simultaneously achieves the advantages of a constant E-field of a parallel-plate sensing area and reduced fabrication requirements of planar structures. Two planar sensing electrodes are separated from a floating electrode through a microfluidic channel to form a 3D capacitive sensing area. A surface coating with a thickness much smaller than the microfluidic channel height prevents direct contact between the MUT and the metal electrodes with minimal impact on sensitivity. As the MUT passes through the capacitive sensing area, the impedance (and hence admittance) of the sensor changes based on the dielectric permittivity of the MUT. At the measurement frequency,  $\omega$ , the admittance of the capacitive sensing area is:

$$Y_s = j\omega C_0(\epsilon_r' - j\epsilon_r''), \quad (1)$$

which can be expressed as:

$$\text{Imag}\left(\frac{Y_s}{\omega}\right) = C_0 \times \epsilon_r', \quad (2)$$

and

$$\text{Real}\left(\frac{Y_s}{\omega}\right) = C_0 \times \epsilon_r'', \quad (3)$$

where  $C_0$  is the nominal, series-connected, air-gap capacitance of the parallel-plate, capacitive sensing area, while  $\epsilon_r'$  and  $\epsilon_r''$  are the real and imaginary parts of the complex relative permittivity of the MUT, respectively.

## III. SENSOR FABRICATION

Fig. 3 shows an illustration of the sensor fabrication and assembly. The sensor substrate is implemented using a commercially available, 0.5mm-thick, Rogers 4350 PCB. The sensing electrodes are designed using the top PCB metal layer and have dimensions of 0.6mm  $\times$  0.6mm with spacing of 0.4mm. A surface-mount, RF connector (MMCX) is soldered onto the back-side of the PCB substrate to form electrical contact and connection to a VNA through a coaxial cable.

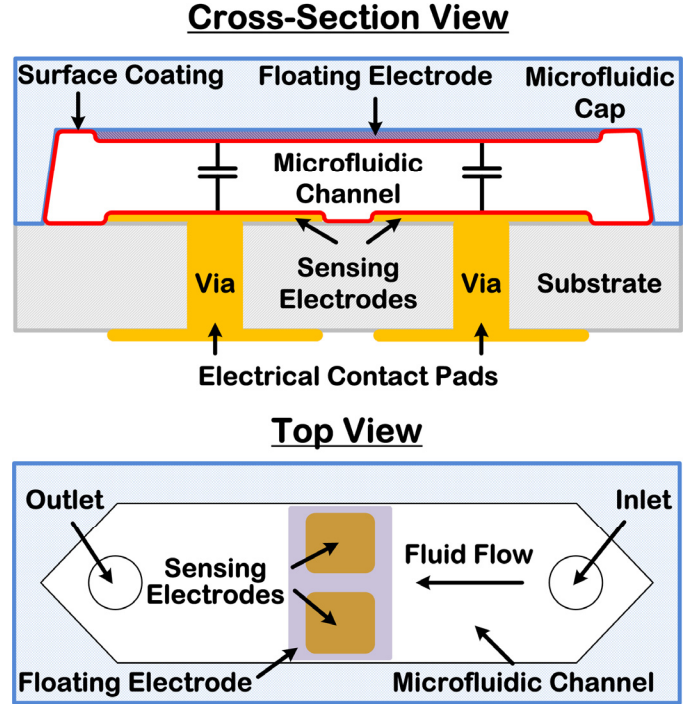


Fig. 2. Cross-sectional and top views of the microfluidic DS sensor based on a 3D capacitive structure with a floating electrode.

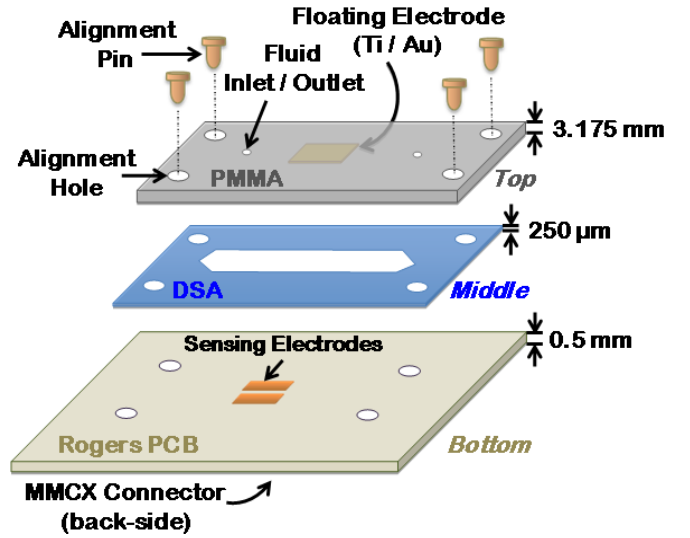


Fig. 3. Illustration of sensor fabrication and assembly. A surface-mount, RF connector is soldered onto the back-side of the PCB substrate (not shown).

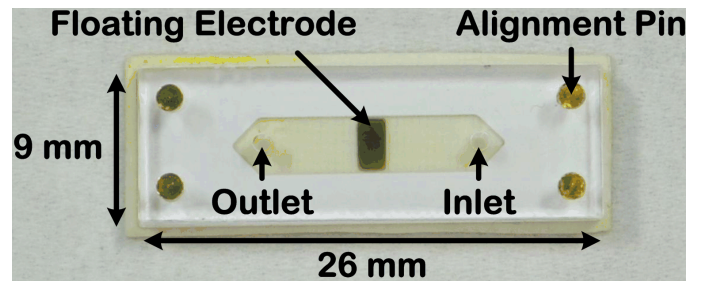


Fig. 4. Photograph of a fabricated sensor prototype.

The microfluidic cap is fabricated by laser micromachining of 3.175mm-thick polymethyl methacrylate (PMMA), and a gold floating electrode with dimensions of 1.2mm × 2.8mm is deposited on the inner top surface of the PMMA cap by sputter deposition of 150-Å/1000-Å Ti/Au using a PMMA shadow mask and lift-off process. A 1.5μm-thick Parylene-N film is then deposited on the surface of the PCB substrate and PMMA cap to protect the metal and plastic surfaces of the sensor from direct contact with the MUT. The microfluidic channel with dimensions of 12mm × 3mm is laser cut into a 250μm-thick double-sided-adhesive (DSA) film. The sensor is then assembled by attaching the PMMA cap to the surface of the PCB substrate using the DSA film, with alignment holes used to align the microfluidic channel and floating electrode over the sensing electrodes. Microfluidic inlet/outlet holes in the PMMA cap are designed with 0.7mm-diameter to fit a standard micropipette tip. The microfluidic channel has a total sample volume of 9μL and a volume of 0.8μL in the sensing area under the floating electrode. Fig. 4 shows a photograph of the fabricated sensor.

#### IV. MEASUREMENT RESULTS

A photograph of the experimental setup is shown in Fig. 5. All calibration and test materials were loaded into the microfluidic channel with a micropipette set to 50μL, and all sensor measurements were conducted in a frequency range of 14MHz to 6.5GHz with a VNA (*Agilent E5071C*) that was used to measure the  $S_{11}$  parameter. The procedure for sensor calibration, measurement of MUT and calculation of  $\epsilon'_r$  and  $\epsilon''_r$  from the  $S_{11}$  measurement is described below.

##### A. Sensor Calibration Using Reference Materials

The sensor was calibrated using six reference materials: air, isopropyl alcohol (IPA), methanol, 1:3 IPA:methanol, 1:1 IPA:methanol and 3:1 IPA:methanol. Each material was first characterized with a commercial dielectric probe kit (*Agilent 85070E*) to obtain a reference permittivity. The calibration material was then loaded into the sensor, and the  $S_{11}$  of the sensor was measured with the VNA. The commercial dielectric probe kit and the VNA set the limits of the calibration frequency range, and therefore the sensor measurement range, to ~14MHz and 6.5GHz, respectively.

An equivalent circuit model of the sensor is shown in Fig. 6, which includes parasitic inductance,  $L_s$ , and capacitance,  $C_{ps}$ , attributed to the PCB vias and MMCX RF connector. An in-circuit calibration procedure is therefore necessary to minimize the effects of these parasitic circuit elements and accurately characterize the admittance of the capacitive sensing area,  $Y_s$ . In Fig. 6,  $Y_{11}$  can be calculated from the measured  $S_{11}$  parameter using (4):

$$Y_{11} = \frac{1}{50\Omega} \times \frac{1 - S_{11}}{1 + S_{11}}. \quad (4)$$

The admittance of the capacitive sensing area,  $Y_s$ , as given in (5), is then de-embedded from the parasitic circuit elements.

$$Y_s = \left( (Y_{11} - j\omega C_{ps})^{-1} - j\omega L_s \right)^{-1}. \quad (5)$$

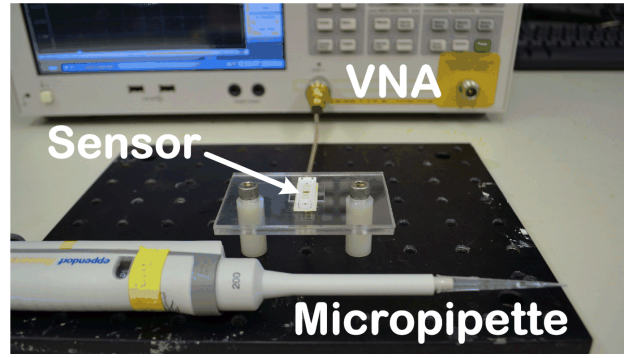


Fig. 5. Photograph of the experimental setup for sensor characterization based on  $S_{11}$  measurement with a VNA.

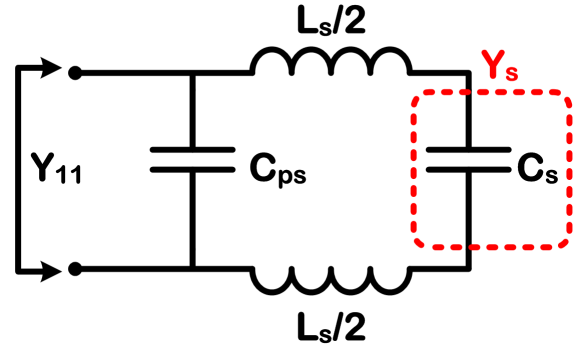


Fig. 6. Equivalent circuit model of the fabricated sensor.

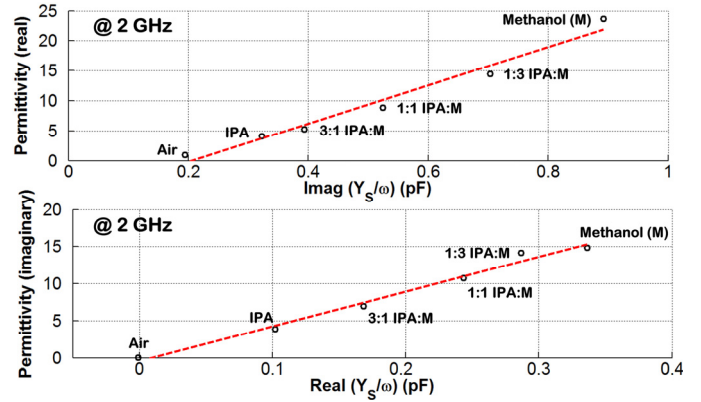


Fig. 7. Calibration plots at 2GHz, relating complex relative permittivity of the calibration materials measured by the dielectric probe kit to sensor measurements. The red dashed line shows a linear fit to the data.

To that end, it can be shown from (2) that  $\text{Imag}\left(\frac{Y_s}{\omega}\right) = C_0$  (i.e., a frequency-independent capacitor) for measurements of air ( $\epsilon'_r = 1$  and  $\epsilon''_r = 0$ ). Sensor measurements with air in the microfluidic channel were thus used to find  $L_s$  and  $C_{ps}$  by sweeping their values and finding optimal values of  $L_s = 1.15\text{nH}$  and  $C_{ps} = 0.24\text{pF}$  such that the variation of  $\text{Imag}\left(\frac{Y_s}{\omega}\right)$  obtained from (5) was minimized versus frequency (i.e., measurement of sensor admittance that most closely resembled that of an ideal air-gap capacitor).

To obtain the complex relative permittivity,  $\epsilon_r$ , of the MUT, a calibration procedure at each measurement frequency point was then performed to relate  $\epsilon_r$  to the de-embedded admittance,  $Y_s$ . Based on (2) and (3), a relationship between  $\epsilon_r$  and  $\frac{Y_s}{\omega}$  can be found by performing a linear least-squares fit between  $\epsilon_r'$  of the calibration materials measured by the dielectric probe kit and  $\text{Imag}\left(\frac{Y_s}{\omega}\right)$  measured by the sensor. Similarly, a linear least-squares fit between  $\epsilon_r''$  of the calibration materials and  $\text{Real}\left(\frac{Y_s}{\omega}\right)$  was also performed. An example calibration plot at 2GHz is shown in Fig. 7.

### B. Measurement of MUT

Ethanol and ethylene glycol were injected into the sensor, and the  $S_{11}$  parameter was measured with the VNA. The de-embedded sensor admittance was calculated, and the linear-fit parameters found in the calibration procedure were used to calculate the corresponding  $\epsilon_r'$  and  $\epsilon_r''$  of each MUT. The sensor measurement results are plotted in Fig. 8 along with reference measurements from *Agilent 85070E* dielectric probe kit (solid lines), demonstrating a very good agreement. The rms errors in  $\epsilon_r'$  and  $\epsilon_r''$  of ethanol over the full frequency range (14MHz to 6.5GHz) were 3.5% and 5.6%, respectively, whereas the corresponding numbers for ethylene glycol were 5.4% and 4.5%, respectively.

## V. CONCLUSION

This paper reported on an RF/microwave microfluidic sensor based on a 3D capacitive sensing area with a floating electrode integrated onto a PMMA microfluidic cap for dielectric spectroscopy. Requiring only an  $S_{11}$  measurement with a vector network analyzer (VNA) and capable of extracting both real and imaginary parts of the complex relative permittivity, the sensor dielectric readings in a frequency range of 14MHz–6.5GHz for ethanol and ethylene glycol agreed very well with bulk-solution reference measurements conducted with an *Agilent 85070E* dielectric probe kit. Our future work will focus on modifying the parasitics de-embedding procedure and sensor calibration algorithm to enable dielectric permittivity extraction using only an  $S_{21}$  measurement of the sensor, which further facilitates replacing the VNA with a custom IC for developing a truly miniaturized platform for dielectric spectroscopy.

## REFERENCES

- [1] F. Kremer, "Dielectric spectroscopy – Yesterday, today and tomorrow," *J. Non-Cryst. Solids*, vol. 305, pp. 1-9, July 2002.
- [2] K. Folgero, T. Friiso, J. Hilland, and T. Tjomslund, "A broadband and high-sensitivity dielectric spectroscopy measurement system for quality determination of low-permittivity fluids," *Meas. Sci. Technol.*, vol. 6, pp. 995-1008, 1995.
- [3] D. A. Robinson, S. B. Jones, J. M. Wraith, D. Or, and S. P. Friedman, "A review of advances in dielectric and electrical conductivity measurement in soils using time-domain reflectometry," *J. Vadose Zone*, vol. 2, pp. 444-475, 2003.

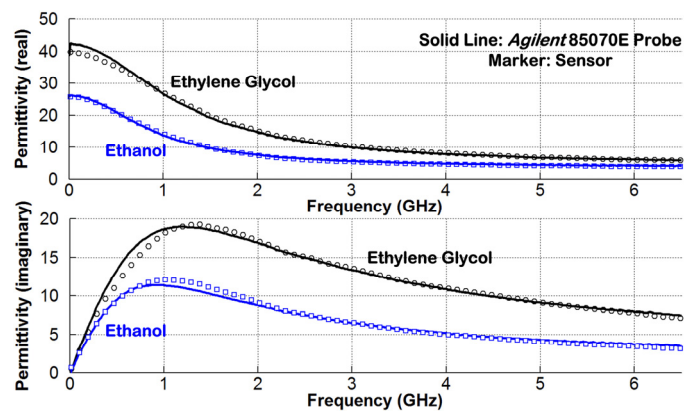


Fig. 8. Complex relative permittivity vs. frequency (14MHz to 6.5GHz) for ethanol and ethylene glycol extracted from  $S_{11}$  measurements by the sensor. Solid lines depict corresponding curves measured with *Agilent 85070E* dielectric probe kit.

- [4] G. Smith, A. P. Duffy, J. Shen, and C. J. Olliff, "Dielectric relaxation spectroscopy and some applications in the pharmaceutical sciences," *J. Pharm. Sci.*, vol. 84, pp. 1029-1044, 1995.
- [5] Y. Hayashi, N. Miura, J. Isobe, N. Shinyashiki, and S. Yagihara, "Molecular dynamics of hinge-bending motion of IgG vanishing with hydrolysis by papain," *J. Biophys.*, vol. 79, pp. 1023-1029, 2000.
- [6] A. Oleinikova, P. Sasisanker, and H. Weingartner, "What can really be learned from dielectric spectroscopy of protein solutions? A case study of ribonuclease A," *J. Phys. Chem. B*, vol. 108, pp. 8467-8474, 2004.
- [7] Y. Feldman, I. Ermolina, and Y. Hayashi, "Time-domain dielectric spectroscopy study of biological systems," *IEEE Trans. Dielect. Elec. Insul.*, vol. 10, pp. 728-753, October 2003.
- [8] S. Abdalla, S. S Al-Ameer, and S. H. Al-Magaishi, "Electrical properties with relaxation through human blood," *Biomicrofluidics*, vol. 4, no. 034101, pp. 1-16, 2010.
- [9] P. Mehta, K. Chand, D. Narayanswamy, D. G. Beetner, R. Zoughi, and W. V. Stoecker, "Microwave reflectometry as a novel diagnostic tool for detection of skin cancers," *IEEE Trans. Instr. Meas.*, vol. 55, pp. 1309-1316, 2006.
- [10] G. R. Facer, D. A. Notterman, and L. L. Sohn, "Dielectric spectroscopy for bioanalysis: From 40 Hz to 26.5 GHz in a microfabricated waveguide," *Appl. Phys. Lett.*, vol. 78, pp. 996-998, February 2001.
- [11] J. C. Booth, N. D. Orloff, J. Mateu, M. Janezic, M. Rinehart, and J. A. Beall, "Quantitative permittivity measurements of nanoliter liquid volumes in microfluidic channels to 40 GHz," *IEEE Trans. Instr. Meas.*, vol. 59, pp. 3279-3288, December 2010.
- [12] A. A. Helmy, H. J. Jeon, Y. C. Lo, A. J. Larsson, R. Kulkarni, J. Kim, J. Silva-Martinez, and K. Entesari, "A self-sustained CMOS microwave chemical sensor using a frequency synthesizer," *IEEE J. Solid-State Circuits*, vol. 47, no. 10, pp. 2467-2483, October 2012.
- [13] M. M. Bajestan, A. A. Helmy, H. Hedayati, and K. Entesari, "A 0.62-10GHz CMOS dielectric spectroscopy system for chemical/biological material characterization," *IEEE MTT-S Int. Microwave Symp. (IMS) Dig.*, Tampa Bay, FL, June 1-6, 2014.
- [14] J. Chien, M. Anwar, E. Yeh, L. P. Lee, and A. M. Niknejad, "A 1-50 GHz dielectric spectroscopy biosensor with integrated receiver front-end in 65nm CMOS," *IEEE MTT-S Int. Microwave Symp. (IMS) Dig.*, Seattle, WA, June 2-7, 2013.
- [15] M. Bakhshiani, M. A. Suster, and P. Mohseni, "A broadband sensor interface IC for miniaturized dielectric spectroscopy from MHz to GHz," *IEEE J. Solid-State Circuits*, vol. 49, no. 8, pp. 1669-1681, August 2014.
- [16] M. A. Suster and P. Mohseni, "An RF/microwave microfluidic sensor based on a center-gapped microstrip line for miniaturized dielectric spectroscopy," *IEEE MTT-S Int. Microwave Symp. (IMS) Dig.*, Seattle, WA, June 2-7, 2013.